

Bull. Astr. Soc. India (2004) **32**, 121–131

## An implementation of transfer-pupil in a spectrograph on optical telescopes

H.K.Das <sup>\*</sup>, Abhay Kohok <sup>†</sup> and S.N.Tandon <sup>‡</sup>

*Inter University Center for Astronomy and Astrophysics (IUCAA), Post Bag 4, Ganeshkhind, Pune - 411 007, India*

Received 6 February 2004; accepted 18 May 2004

**Abstract.** Based on the transfer pupil technique we develop a method to measure the lower order aberration coefficients for optical telescopes; the method makes use of a Hartmann mask in a spectrograph for sampling the wavefront at different locations.

### 1. Introduction

One of the most common methods used for monitoring optics of Cassegrain telescopes is to sample the wavefront, as obtained by a long time integration of a stellar image, by a screen and measuring the slopes of the individual sampled portions. The classical Hartmann test uses a full-size screen placed above the secondary mirror ( or outside the prime focus) of the telescope; this technique is no more in common use, (Wilson II, P150). An equivalent technique, of measurements on transfer-pupil, is capable of making accurate measurements by using smaller components placed at the telescope focus, see for example (Wilson II, 1999 P 150-151 and Wilson et al. 1984) for an implementation of the technique in a spectrograph.

In the commonly used version of transfer-pupil scheme the screen (perforated mask) is usually an array of lenslets – this is the Shack Hartmann mask (Platt et al. 1971, Shack et al. 1971) . Each lenslet forms a sub-aperture of the transferred pupil and images it on the detector. In this paper, we describe an equivalent scheme in which a screen placed on a low power lens is used, instead of the array of lenslets; in this process we might be using only a small fraction of the total light available, but it is much simpler to implement.

---

<sup>\*</sup>e-mail:hkdas@iucaa.ernet.in

<sup>†</sup>e-mail:abhay@iucaa.ernet.in

<sup>‡</sup>e-mail:sntandon@iucaa.ernet.in

In section 2 details of the optical arrangement is described , and in section 3 complete procedure used to calculate decenter and defocus of the telescope is described. In section 4 we describe the analysis part, and Appendix I describes the main algorithm of the computer codes developed to analyze the images and also highlights a laboratory set up for testing the procedure.

## 2. Experimental Set Up

To transfer the pupil of the telescope we would use the IUCAA faint object spectrograph and camera (IFOSC), (R. Gupta et al. 2002); the pupil of the telescope is transferred on to the grism wheel. The pupil size here is about 32 mm; see Fig.1. The set up is made for use with IUCAA 2-m telescope which is under installation.

The observational procedure is as follows; an image of a suitably chosen star is obtained at the telescope focus. The  $f/10$  beam from the telescope then meets the collimator (316 mm focal length) which images the exit pupil of the telescope on the grism wheel, where a perforated mask is mounted; please refer Fig.1. The collimated beam (from the collimator) illuminates the perforated mask, and is finally imaged by the camera (142 mm focal length) on the detector.

A similar image is then obtained by illuminating a pinhole (mounted on the aperture wheel) with a light source in the calibration unit (explained below); the two images are then compared to obtain the aberration coefficients, as explained in section 4.

In the laboratory we used the  $f/10$  light from the calibration unit of IFOSC (not shown in Fig.1). The calibration unit is an extra unit of IFOSC; it simulates the exit pupil of the IUCAA telescope which produces an  $f/10$  beam, including the obscuration due to the secondary mirror.

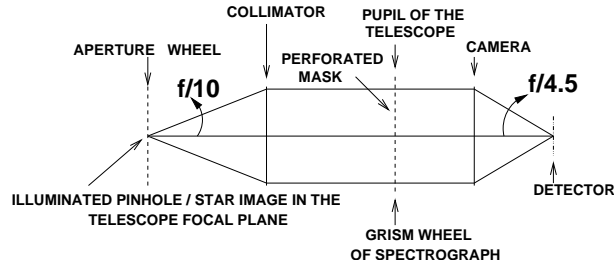


**Figure 1.** The position of the transferred pupil of the telescope in the grism wheel of the spectrograph is shown.

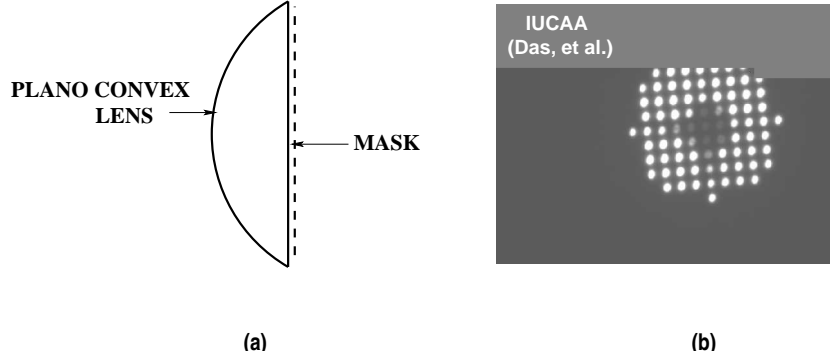


**Figure 2.** (a) The perforated mask on the lens of diameter 40 mm, the holes are in a circle of 30 mm diameter; (b) Images of the pinhole on the detector.

As shown in Fig. 2a, the perforated mask is placed on a plano convex lens, of focal length 1000 mm, and the entire assembly is mounted on the grism wheel of IFOSC; the mask is made of a 50 micron copper foil and it contains 1 mm diameter holes on a grid of 3X3 mm placed on a circle of 30 mm diameter. The lens slightly decollimates the collimated beam, and images of the pin-hole are therefore separated from each other as shown in Fig.2b.

### 3. Procedure of obtaining decentering and defocus

#### 3.1 Finding the aberration coefficients

The main idea of wavefront analysis is that local tilts in the wavefront would cause the light ray to reach a point away from the point where the light ray would have reached had it been an ideal wavefront. So an optical arrangement (Hartmann mask) is introduced to monitor tilts in different parts of the wavefront. Comparison of the ideal and aberrated wavefront would give us an estimate of the wavefront tilts.

The wavefront aberration  $W$ , used in this analysis can be represented as (Wilson II p-148,284):

$$W = K_{11}\rho\cos(\phi + \theta_{11}) + K_{02}\rho^2 + K_{13}\rho^3\cos(\phi + \theta_{13}) + K_{04}\rho^4 \quad (1)$$

where we have considered only lower order terms. In Eqn.1,  $\rho$  is the radial distance of the holes of the perforated mask from the center normalized to unity at the edge,  $K_{nm}$  is the optical aberration coefficient,  $\phi$  the azimuth angle in the pupil plane,  $\theta_{nm}$  the phase angle of the aberration and  $n,m$  are positive integers. The different terms,  $K_{11}\rho\cos(\phi + \theta_{11})$  corresponds to wavefront tilt,  $K_{02}\rho^2$  corresponds to defocus,  $K_{13}\rho^3\cos(\phi + \theta_{13})$  corresponds to decentering coma and  $K_{04}\rho^4$  to spherical aberration.

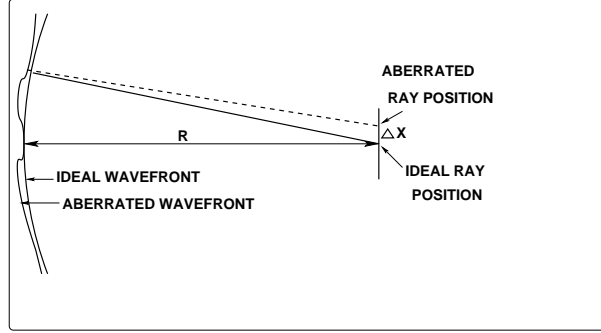


**Figure 3.** Figure showing the actual and the ideal ray position.

From Eqn.1, the wavefront slopes can be obtained as,

$$W'_x = K_{11}\cos\theta_{11} + 2K_{02}x + 3K_{13}x^2\cos\theta_{13} - 2K_{13}xysin\theta_{13} + K_{13}y^2\cos\theta_{13} + 4K_{04}x^3 + 4K_{04}xy^2 \quad (2)$$

$$W'_y = -K_{11}\sin\theta_{11} + 2K_{02}y - K_{13}x^2\sin\theta_{13} + 2K_{13}xycos\theta_{13} - 3K_{13}y^2\sin\theta_{13} + 4K_{04}x^2y + 4K_{04}y^3 \quad (3)$$

where  $W'_x = \Delta x/R$ ,  $W'_y = \Delta y/R$ , (Malacara and Fig.3);  $x$  and  $y$  are the cartesian components of  $\rho$ ,  $\rho\cos\phi$  and  $\rho\sin\phi$ ;  $\Delta x$  and  $\Delta y$  are the shifts in the centroids of the pinhole images between the ideal and the aberrated image and  $R$  is the focal length of the lens which re-images the pupil.

In order to find solution to these equations using a linear least square fit to the images, a parametrization is done as follows:

$$\Delta x/R = a_1 + b_1x + c_1(3x^2 + y^2) + 2d_1xy + e_1(x^3 + xy^2) \quad (4)$$

$$\Delta y/R = a_2 + b_1y + 2c_1xy + d_1(x^2 + 3y^2) + e_1(x^2y + y^3) \quad (5)$$

where,  $a_1 = K_{11}\cos\theta_{11}$ ,  $a_2 = -K_{11}\sin\theta_{11}$ ,  $b_1 = 2K_{02}$ ,  $c_1 = K_{13}\cos\theta_{13}$ ,  $d_1 = -K_{13}\sin\theta_{13}$ ,  $e_1 = 4K_{04}$

The aberration coefficients ( $K$ s) and phase angles ( $\theta$ s) can be obtained in terms of  $a, b, c, d, e$  as follows:

$$K_{11} = \sqrt{a_1^2 + a_2^2}, \quad K_{02} = b_1/2, \quad K_{13} = \sqrt{c_1^2 + d_1^2}, \quad K_{04} = e_1/4, \quad \sin\theta_{11} = -a_2/K_{11}, \quad \sin\theta_{13} = -d_1/K_{13}, \quad \cos\theta_{11} = a_1/K_{11}, \quad \cos\theta_{13} = c_1/K_{13}$$

### 3.2 Finding decentering

The decentering coma can be equated to the lateral tangential Coma by equating  $K_{13}$  to

$$-3/d_1(y_1/r_1)^2[1 + (1 - 2d_1/r_1)(\mu_2^2 - 1)]\delta \quad \text{in radians} \quad (6)$$

(Wilson I, p 253), where  $y_1$  is the half diameter of the primary,  $r_1$  is the radius of curvature of the primary,  $d_1$  is the distance between primary and secondary,  $\mu_2$  is the inverse of the magnification by the secondary, and  $\delta$  is the decentering (in mm) of the secondary mirror with respect to the primary. From known values of  $y_1$ ,  $r_1$ ,  $d_1$ , and  $m_2$  and measured  $K_{13}$  decentering can be calculated.

As the effect of angular decenter of the secondary is usually small compared to that of lateral decentering (Wilson I, sec. 3.7.2.1 and 3.7.2.2), we only consider decentering.

### 3.3 Finding defocus

$$\text{The defocus in mm} = -b_1 R^2 / (\text{pupil radius}) \quad (7)$$

where ‘‘pupil radius’’ is the radius of the reimaged pupil in mm.

## 4. Analysis

We need a set of two images (as in Fig. 2b) for our analysis; (a) an ideal image obtained by illuminating a pinhole at the focal plane and (b) an image obtained with a long time (> 20 secs.) exposure to a suitable star.

These two images need to be compared to obtain the wavefront deviations, i.e.  $\Delta x$  and  $\Delta y$  in Eqns. 4 and 5. To solve these equations computer programs were developed in IDL programming language. The IDL program does the following.

1. Calculates the centroids of all the pin holes from the ideal and aberrated images.
2. Calculates  $\Delta x$  and  $\Delta y$  of the two set of centroids.
3. Obtains the coefficients,  $a_1, a_2, b_1, c_1, d_1$  and  $e_1$  by the method of least square fit.
4. Interprets these different coefficients in terms of the aberration coefficients.
5. Calculates decenter and defocus.

For a discussion on the results obtained in a simulation experiment and their interpretation please refer to Appendix I.

## 5. Conclusion

In this paper we have described the theory, experimental method and analysis techniques to measure the decenter and defocus of large optical telescopes through the use of a Hartmann mask placed in the collimated beam of a focal plane instrument.

## 6. Acknowledgment

We are thankful to Paramita Barai of IIT Kharagpur, who had initially worked on this problem as our project student.

## References

- Gupta R., et al., 2002, *BASI*, **30**, 785.  
Malacara Daniel, 1978, *Optical Shop testing*, Wiley, New York, p. 326.  
Platt B., Shack R.V., 1971, Optical sciences center newsletter, Univ. of Arizona, Tucson, **5**(1), 15.  
Shack R.V., Platt B.C., 1971, *JOSA*, **61**, 656.  
Wilson R.N., 1996, *Reflection telescope optics I*, A&A Library, Berlin, Springer-Verlag, New York.  
Wilson R.N., 1999, *Reflection telescope optics II*, A&A Library, Berlin, Springer-Verlag, New York.  
Wilson R.N., Franza F., Noethe L., Tarengi M., 1984, in Proc. IAU colloq. No.79: Very Large telescopes, their Instrumentation and Programs, ESO, Garching, 119.

## Appendix I

### A.1 Brief description of the main program

The main program needs the following parameter files and a subroutine:

- A parameter file for calculating the centroids. This file contains the following parameters; background, minimum good data, maximum good data, small box size, big box size.
- A parameter file for reading the ideal and aberrated image names and the rough coordinates of both the images; (these rough coordinates are used to calculate the centroids).
- A parameter file for the telescope and CCD parameters; it contains the pixel size in mm, magnification by CCD in pixel/mm, focal length of the camera lens of IFOSC, pupil radius in pixels, radius of the primary mirror, in mm, radius of curvature of the primary mirror in mm, distance between primary and secondary mirror, in mm, and magnification by secondary mirror.
- A subroutine for calculating the centroid, (flowchart given in Fig.4).

### A.2 Laboratory set up for testing the procedure

To test the validity of the analysis technique, and also to test the codes developed, we illuminated the pinhole with white light from the calibration unit, as explained in section 2. Two images of the pinhole were taken as described below; the images appear as shown in Fig. 2b.

- First image - camera lens of IFOSC focused: Ideal wavefront.
- Second image - camera lens of IFOSC shifted by  $100 \mu\text{m}$ : Aberrated wavefront; a check on raytracing with Zeemax software shows that this shift of  $100\mu\text{m}$  corresponds to a defocus of  $140\mu\text{m}$ .

These two images were analyzed on the basis of the program in Fig.5.

The test results obtained are as follows:

$$\begin{aligned}
 a_1 &= 1.66e - 05 \\
 a_2 &= -3.46e - 05 \\
 b_1 &= -9.2e - 05 \\
 c_1 &= 1.32e - 06
 \end{aligned}$$

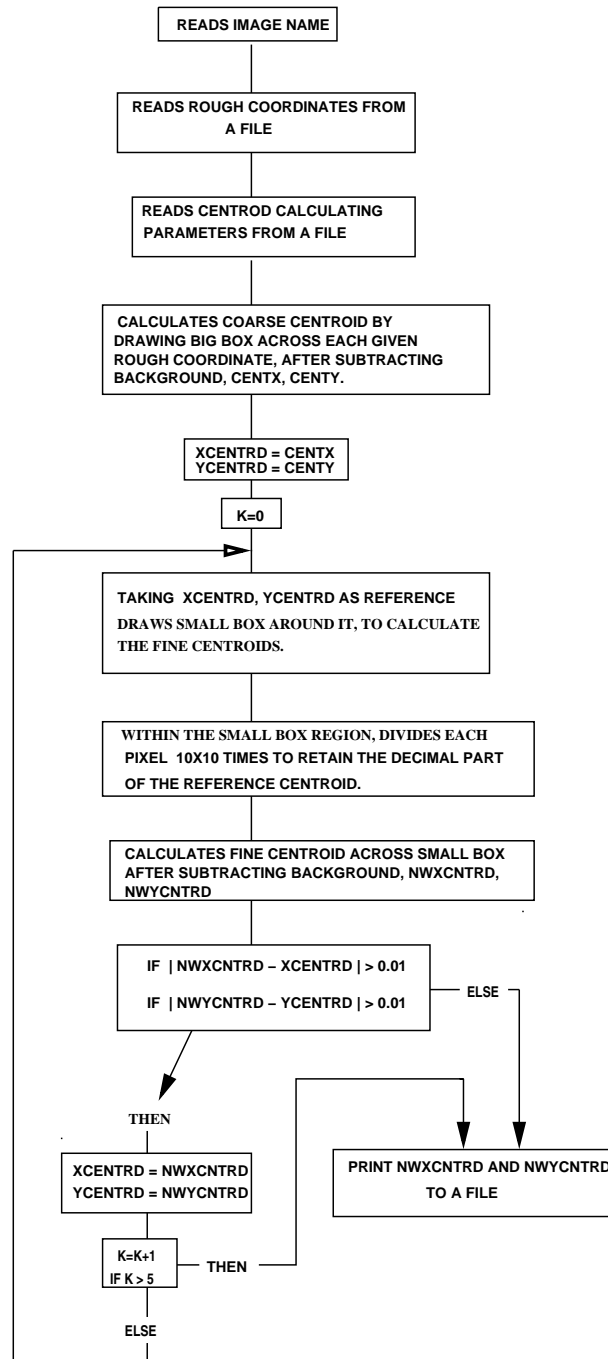


Figure 4. Flow chart of the centroid calculating program.



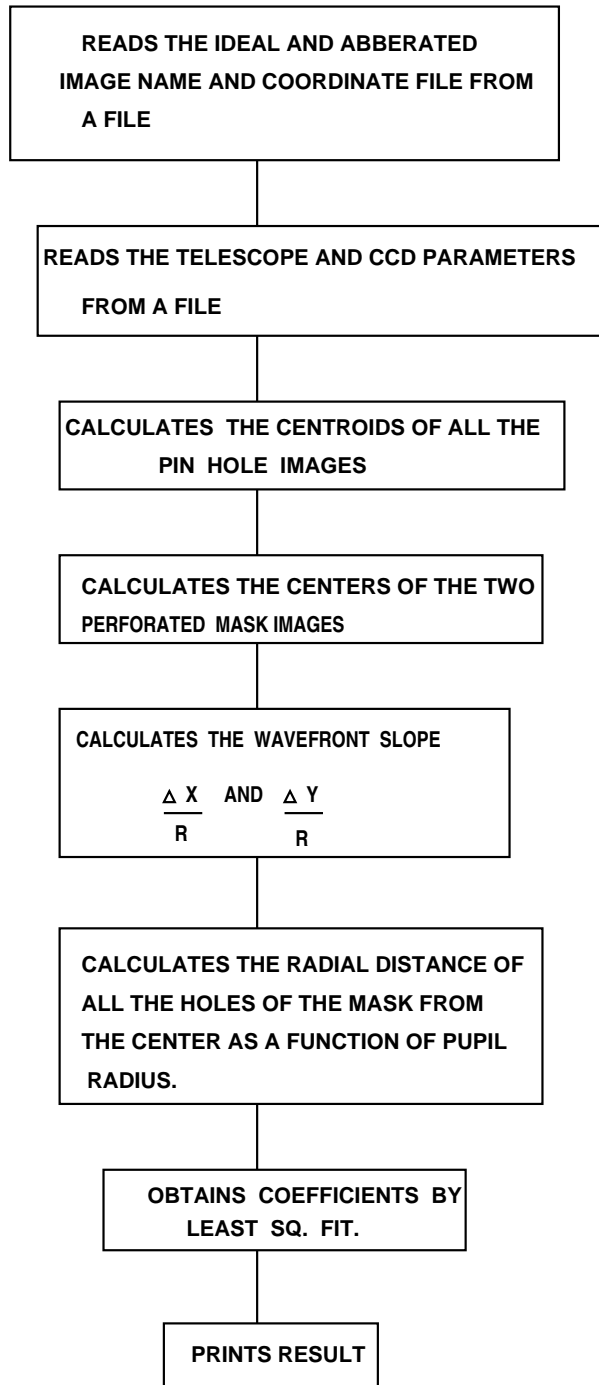


Figure 5. Flow chart of the main wavefront calculating program.

$$\begin{aligned} d_1 &= 4.46e - 07 \\ e_1 &= -2.94e - 06 \end{aligned} \tag{8}$$

$K_{11}$  (TILT, in rad.) is 3.84e-05  
 Tilt\_az(deg.)( $\theta_{11}$ ) is 64.32  
 $K_{02}$  (DEFOCUS, in rad.) is -4.6e-05  
 Defocus(mm) is 0.12  
 $K_{13}$ (DECENTRING COMA,in rad.) is 1.40e-06  
 Secondary decenter(in mm) is 0.39  
 Coma\_az(deg.)( $\theta_{13}$ ) is -18.61  
 $K_{04}$  (3rd ORDER SPHERICAL ABERRATION, in rad.) is -7.35e-07

Let us try to understand the value of each coefficient listed above with reference to the situation that the experiment only involved a defocus.

- **Defocus:** As explained earlier the expected defocus is 0.14 mm, whereas a value of 0.12 mm is obtained; this error of  $20\mu\text{m}$  would deteriorate the image quality by  $\approx 4\mu\text{m}$  for our f/4.5 camera lens, which corresponds to  $0.09''$  in the telescope focal plane.
- **Tilt:** The returned value of tilt corresponds to a shift of  $\approx 5\mu\text{m}$  on the CCD, which corresponds to  $0.1''$  on the telescope focal plane.  
 We know from our previous testing of IFOSC that the focus adjustment of the camera has some lateral movements associated with it, and this could be the source of it.
- **Decentering Coma:** In the linear scale this error is  $0.2\ \mu\text{m}$  (0.013 pixel) corresponding to  $0.005''$  in the telescope focal plane, whereas the expected value is nil. The value returned represents error in the method.
- **Spherical aberration:** In the linear scale this error is  $0.1\ \mu\text{m}$  (0.007 pixel) corresponding to  $0.002''$  in the telescope focal plane, whereas the expected value is nil. The value returned represents error in the method.

### A.3 Error estimate of the coefficients

To estimate the error level in the coefficients given in Eqn.8, and also the  $K_{nm}$  coefficients, we did the following. We added normally distributed random numbers to the values of  $\Delta x$  and  $\Delta y$  (please refer Eqns.4 and 5); as our error in the measurement of the centroids was 0.01 pixel, the rms value of the random numbers was chosen at 0.02 and the values of the coefficients calculated. This procedure was repeated 30 times and the

rms error on the coefficients was found from these 30 trials. The rms error on the  $K_{nm}$  coefficients are in the range  $3 - 5 \times 10^{-7}$  radians; i.e. the errors in the CCD image plane are  $\sim 0.1''$  which corresponds to  $< 0.003''$  in the focal plane of the telescope.